Following the Formation of Supported Lipid Bilayers on Mica: A Study Combining AFM, QCM-D, and Ellipsometry

Ralf P. Richter and Alain R. Brisson
Laboratoire d'Imagerie Moléculaire et Nano-Bio-Technologie, IECB, UMR-CNRS 5471, Université Bordeaux I, 33607 Pessac Cedex, France

ABSTRACT Supported lipid bilayers (SLBs) are popular models of cell membranes with potential biotechnological applications and an understanding of the mechanisms of SLB formation is now emerging. Here we characterize, by combining atomic force microscopy, quartz crystal microbalance with dissipation monitoring, and ellipsometry, the formation of SLBs on mica from sonicated unilamellar vesicles using mixtures of zwitterionic, negatively and positively charged lipids. The results are compared with those we reported previously on silica. As on silica, electrostatic interactions were found to determine the pathway of lipid deposition. However, fundamental differences in the stability of surface-bound vesicles and the mobility of SLB patches were observed, and point out the determining role of the solid support in the SLB-formation process. The presence of calcium was found to have a much more pronounced influence on the lipid deposition process on mica than on silica. Our results indicate a specific calcium-mediated interaction between dioleoylphosphatidylserine molecules and mica. In addition, we show that the use of PLL-*g*-PEG modified tips considerably improves the AFM imaging of surface-bound vesicles and bilayer patches and evaluate the effects of the AFM tip on the apparent size and shape of these soft structures.

INTRODUCTION

Supported lipid bilayers (SLBs), formed by the spreading of vesicles from solution (Watts et al., 1984; McConnell et al., 1986), have already found widespread use as mimics of cell membranes (Watts et al., 1984; Sackmann, 1996; Salafsky et al., 1996; Reviakine et al., 1998; Milhiet et al., 2002; Yip et al., 2002) and are attractive as building blocks for biotechnological applications (Sackmann, 1996; Boxer, 2000; Reviakine and Brisson, 2001; Kam and Boxer, 2003; Larsson et al., 2003). It is only in the recent years that a detailed image of the structural intermediates of the formation of SLBs is emerging from both experimental (Rädler et al., 1995; Keller and Kasemo, 1998; Jass et al., 2000; Keller et al., 2000; Reviakine and Brisson, 2000; Johnson et al., 2002; Reimhult et al., 2003; Richter et al., 2003; Benes et al., 2004) and theoretical studies (Seifert and Lipowsky, 1990; Seifert, 1997; Zhdanov et al., 2000), though many issues about the formation of SLBs remain to be explored. We do not have, at present, a comprehensive understanding of the driving forces of the SLB-formation process (Nollert et al., 1995; Reviakine and Brisson, 2000; Zhdanov and Kasemo, 2001; Reimhult et al., 2002b; Richter et al., 2003). In particular, the role of the solid support in the rupture of vesicles and the promotion of SLB formation (Keller and Kasemo, 1998; Starr and Thompson, 2000; Reimhult et al., 2003; Richter and Brisson, 2004) remains poorly understood.

Silica-based surfaces and mica are the prototypes of solid supports that are currently used to form solid-supported lipid bilayers. Notably, previous studies have provided indications for some differences in the SLB-formation process on these supports, such as the role of calcium (Reviakine and Brisson, 2000; Richter et al., 2003) and the influence of the vesicle size on rupture (Reviakine and Brisson, 2000; Reimhult et al., 2002b). A detailed comparison of the SLB-formation process between these surfaces is, however, still lacking.

A multitude of techniques, such as fluorescence microscopy (Nollert et al., 1995; Johnson et al., 2002), quartz-crystal microbalance with dissipation monitoring (QCM-D) (Keller and Kasemo, 1998; Keller et al., 2000; Reimhult et al., 2002a,b, 2003; Richter et al., 2003; Seantier et al., 2004), atomic force microscopy (AFM) (Jass et al., 2000; Reviakine and Brisson, 2000; Richter et al., 2003; Tokumasu et al., 2003; Seantier et al., 2004), surface plasmon resonance (SPR) (Keller et al., 2000), and ellipsometry (Benes et al., 2004) has been used to investigate the SLB-formation process. We have recently illustrated the complementary nature of AFM and QCM-D for the analysis of vesicle adsorption and SLB formation on silica (Richter et al., 2003). Giving access to spatially resolved structural information on the nanometer scale and overall adsorption and reorganization dynamics, respectively, the combination of both techniques has enabled the identification and characterization of several different SLB-formation pathways stressing the importance of electrostatic interactions in the SLB-formation process. Others have pointed out the complementary aspects between QCM-D and optical surface-sensitive methods, such as SPR (Keller et al., 2000) or ellipsometry: while optical methods allow measuring the dry mass of the adsorbed lipids, QCM-D provides not only the hydrated mass, but also a direct mean (the dissipation) to distinguish between different phases of the adsorbate—surface-bound vesicles or bilayer patches (Keller

Submitted September 28, 2004, and accepted for publication February 14, 2005.

Address reprint requests to Alain R. Brisson, E-mail: a.brisson@iecb.u-bordeaux.fr.

0006-3495/05/05/3422/12 $2.00

doi: 10.1529/biophysj.104.053728

et al., 2000). As such, the combination of QCM-D and SPR has allowed establishing the concept of local critical vesicular coverage (Keller et al., 2000). Recent work has also demonstrated that in situ measurements on mica can be performed both with ellipsometry (Benes et al., 2002) and with QCM-D (Richter and Brisson, 2004) in a reproducible manner, opening up for the joint use of QCM-D, ellipsometry, and AFM on this support.

In this study, we combine sequential measurements by QCM-D and AFM on identical supports, complemented by ellipsometry, to characterize the vesicle adsorption and the SLB formation on mica. As in a previous study on silica (Richter et al., 2003), we employ vesicles with varying net charges, from positively charged dioleoyltriammonium-propane (DOTAP) to mixtures of zwitterionic dioleoylphosphatidylcholine (DOPC) and negatively charged dioleoylphosphatidylserine (DOPS). This allows for a quantitative comparison between the lipid deposition on mica and on silica and gives new insight in the role of the solid support, the lipid composition of the vesicles, and the calcium-EDTA balance in the SLB-formation process.

MATERIALS AND METHODS

Materials

Dioleoylphosphatidylcholine (DOPC), dioleoylphosphatidylserine (DOPS), and dioleoyltrimethylammonium-propane (DOTAP) were purchased from Avanti Polar-Lipids (Alabaster, AL). Lyophilized poly(L-lysine)-*g*-poly(ethylene glycol) (PLL-*g*-PEG) with a 20-kDa poly(L-lysine)-backbone, side chains of 2 kDa poly(ethylene glycol), and a grafting ratio of $g = 3.4$ (Huang et al., 2002) was synthesized and kindly provided by the group of M. Textor (ETH, Zurich, Switzerland). Other chemicals were purchased from Sigma (St. Louis, MO). Ultrapure water with a resistivity of 18.2 MΩ was used (Maxima, USF ELGA, Trappes, France).

Muscovite mica disks of 12 mm diameter were purchased from Metafix (Montdidier, France). QCM-D sensor crystals (5 MHz), reactively sputter-coated with 50 nm silicon oxide, were purchased from Q-SENSE (Gothenburg, Sweden). Low-viscosity epoxy glue (EPOTEK 377) for the mica gluing was purchased from Gentec Benelux (Waterloo, Belgium).

A buffer solution made of 150 mM NaCl, 3 mM NaN_3, and 10 mM HEPES, pH 7.4, was prepared in ultrapure water, and either 2 mM EDTA or 2 mM $CaCl_2$ were added as indicated in the text. Small unilamellar vesicles (SUVs) of desired lipid mixture were prepared by sonication as described earlier (Richter et al., 2003). Before use, vesicle suspensions were diluted to 0.1 mg/mL if not otherwise stated.

Quartz crystal microbalance with dissipation monitoring (QCM-D)

QCM-D measurements (Rodahl et al., 1995) were performed with the Q-SENSE D300 system equipped with an Axial Flow Chamber (QAFC 302) (Q-SENSE). Briefly, upon interaction of (soft) matter with the surface of a sensor crystal, changes in the resonance frequency, f, related to attached mass (including coupled water), and in the dissipation, D, related to frictional (viscous) losses in the adlayer are measured with a time resolution of better than 1 s.

The QCM-D sensor crystals were coated with mica and verified to operate stably and reliably according to a previously described protocol (Richter and Brisson, 2004). Briefly, mica sheets were glued to the QCM-D sensors using epoxy glue. The glued mica sheets were cleaved until sufficiently thin mica layers and stably operating sensors were obtained.

Measurements were performed in exchange mode (Richter et al., 2003), if not otherwise stated. The exchange mode allows following processes of adsorption and surface adlayer changes in situ while sequentially exposing different solutions to the supports. In this mode the fluid in the measurement chamber is generally still. Occasionally, flow mode was employed, i.e., the solution was continuously delivered to the measurement chamber (flow speed 80 μL/min) by the aid of a peristaltic pump (ISM832A, Ismatec, Zürich, Switzerland) (Richter et al., 2005). Resonance frequency and dissipation were measured at several harmonics (15, 25, 35 MHz) simultaneously. The working temperature was 24°C.

If not stated otherwise, changes in dissipation and in normalized frequency ($\Delta f_{norm} = \Delta f_n/n$, with n being the overtone number) of the third overtone ($n = 3$, i.e., 15 MHz) are presented. Adsorbed masses, Δm, are calculated according to the Sauerbrey equation (Sauerbrey, 1959), $\Delta m = -C\Delta f_{norm}$, with the mass sensitivity constant $C = 17.7\ ng\cdot cm^{-2}\cdot Hz^{-1}$ for 5 MHz sensor crystals. The equation has been demonstrated to be valid, within 5% error, for lipid bilayers or adsorbed nonruptured SUVs on rigid sensor coatings with a thickness ranging from several nanometers (such as evaporated gold or sputtered silica; Keller and Kasemo, 1998; Reimhult et al., 2002b) to several micrometers (such as glued mica sheets; Richter and Brisson, 2004).

For transfer of QCM-D sensors with adsorbed material from the QCM-D chamber to the AFM, the sensors were unmounted with the aid of a suction holder (Meni CUP, Menicon Pharma, Illkirch-Graffenstaden, France), ensuring that the sample remained permanently covered with liquid.

Ellipsometry

Ellipsometry is an optical technique based on the measurement of changes in the ellipsometric angles, Δ and Ψ (Cuypers et al., 1983; Tompkins, 1993), of elliptically polarized light upon reflection off a planar surface. These changes are sensitive to the presence of thin deposited films and, consequently, the method allows monitoring adsorption phenomena in situ, at the solid-liquid interface, with a mass resolution in the range of 5–10 $ng\cdot cm^{-2}$. The employed null-ellipsometer setup has a time resolution of 10–15 s and is described in detail elsewhere (Cuypers et al., 1983; Corsel et al., 1986). In this study we consider the change in the angle Δ only, which is roughly proportional to the (dry) lipid mass adsorbed to mica (Benes et al., 2004).

Measurements were performed in an open cuvette system (Corsel et al., 1986), at room temperature. Mica disks were glued on an aluminum slide over a hole (8 mm diameter) using melted wax (Benes et al., 2002). The backside of the mica disks was rendered opaque with emery paper before gluing onto the aluminum slide. Uniform mica surfaces were obtained by cleavage of the front side with adhesive tape and immediately mounted in the buffer-filled cuvette. The buffer (~3 mL) was stirred with a magnetic stirrer (~1000 rpm). Samples were pipetted at appropriate concentrations into the buffer. Rinsing was realized by injecting ~30 mL of buffer (injection rate, ~1 mL/s) while simultaneously withdrawing excess liquid.

Preparation of PLL-*g*-PEG-coated AFM tips

Oxide-sharpened silicon nitride cantilevers with a nominal spring constant of 0.06 N/m (Digital Instruments, Santa Barbara, CA) were rinsed in water and ethanol, blow-dried with nitrogen, and exposed to ultraviolet/ozone (BHK, Claremont, CA) for 10 min (Richter et al., 2003). The cleaned tips were transferred immediately into a solution of 1 mg/mL PLL-*g*-PEG in 10 mM HEPES, pH 7.4. After 30 min of immersion, the tips were withdrawn, rinsed with ultrapure water, and blow-dried with nitrogen. PLL-*g*-PEG-modified tips were stored on Gel-Pak (Scotch, CA) under nitrogen and used within four weeks.

Atomic force microscopy

AFM measurements were performed in liquid using a Nanoscope IV-Multimode (Veeco, Dourdan, France), equipped with a J-scanner (120 μm).

Before use, the tapping mode fluid cell was washed in successive baths of ethanol and ultrapure water, followed by extensive rinsing in ethanol and blow-drying in a stream of nitrogen. Tubings and O-ring were sonicated in ethanol and water, rinsed with ethanol, and blow-dried in nitrogen.

For AFM investigations subsequent to QCM-D measurements, mica-coated QCM-D sensors, covered with the sample, were attached to Teflon-coated (Bytac, Norton, OH) metal disks using double-sided tape (TESA, Hamburg, Germany) and installed on the AFM scanner. In all other cases, mica disks were glued to Teflon-coated metal disks using the epoxy glue. Uniform surfaces were obtained by cleavage with adhesive tape and immediately covered with buffer solution. The AFM was equilibrated for 5–30 min before imaging.

Images were recorded in contact mode or tapping mode as indicated. Contact mode images were acquired at scanning rates of 4–8 Hz while manually adjusting the force to a minimum (<200 pN). Tapping mode images were acquired at scanning rates of 1–2 Hz. A resonance frequency ~7 kHz was chosen with low free amplitude (0.4–0.6 V) and minimum load upon scanning. Images were first-order plane-fitted except otherwise stated.

RESULTS

The formation of SLBs from SUVs made of DOPC and DOPS (molar ratio 4:1) in 2 mM $CaCl_2$ has already been well characterized by QCM-D on silica (Richter et al., 2003), and to some extent by AFM on mica (Reviakine and Brisson, 2000), and was chosen as a reference system in our study. The overall kinetics of the SLB-formation process on mica by QCM-D (Fig. 1) reveals a two-phase behavior. In the first phase the frequency decreases beyond -25 Hz ($\Delta f_{min} = -39$ Hz) whereas the dissipation increases ($\Delta D_{max} = 1.6 \times 10^{-6}$), evidencing the adsorption of a substantial amount of nonruptured vesicles. Final shifts in frequency ($\Delta f_{fin} = -25$ Hz) and dissipation ($\Delta D_{fin} < 0.2 \times 10^{-6}$) after the second phase match values previously obtained on silica (Keller and Kasemo, 1998; Richter et al., 2003) and indicate the presence of an SLB. AFM imaging of the final state of the surface adlayer revealed a flat surface devoid of defects on areas of 25 μm^2 and more and confirmed the presence of a confluent ideal bilayer (Fig. 6 *B*).

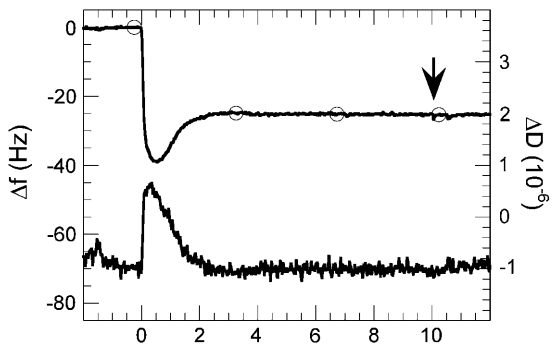

FIGURE 1 QCM-D response, i.e., changes in frequency (–○–) and dissipation (*solid line*), for the deposition of SUVs composed of DOPC/DOPS (molar ratio 4:1) on mica in 2 mM $CaCl_2$. Lipid exposure starts at 0 min. The peak in dissipation and the minimum in frequency indicate the presence of intact vesicles bound at an intermediate state. The final frequency shift of -25 Hz and the low final dissipation shift indicate the presence of an SLB. A rinse with buffer (*arrow*) does not affect the SLB.

The early phase of SLB formation

In some measurements, the SLB-formation process was interrupted by rinsing with buffer at an early stage, i.e., long before the maximum in dissipation and minimum in frequency were reached (Fig. 2 *A*). As the surface coverage is low, interactions between vesicles are expected to be negligible and hence the stability of isolated vesicles can be investigated. After rinsing, the frequency slowly increased and the dissipation slowly decreased, indicating that vesicles are not stable. AFM images of the surface 1 h after rinsing (Fig. 2, *B* and *C*) revealed the presence of two types of objects, identified as immobilized vesicles and bilayer patches, respectively, from their apparent shapes and heights (Reviakine and Brisson, 2000; Richter et al., 2003). We believe that the distribution of vesicles and bilayer patches revealed in the image closely resembles the true distribution and is not significantly altered by the imaging process (see also below).

The smallest vesicles and bilayer patches had an apparent diameter of ~25 and ~28 nm (for details of the size determination see the Supplementary Material), respectively, close to the size expected from SUVs. Notably, the size of both vesicles and SLB patches was heterogeneous, i.e., both small and large patches and vesicles were present, indicating a rather weak dependence of the rupture tendency on the vesicle size over the size distribution observed here. In general, lipid patches exhibited a circular shape.

Both vesicles and bilayer patches were found not to move laterally over the time range of 10 min and more, except at relatively high imaging forces. AFM images acquired at low lipid coverage (c.f. Fig. 2 *B*) did only exceptionally, presumably due to tip artifacts, reveal vesicles or bilayer patches that disappeared upon imaging.

To verify whether lipid material desorbs from the mica surface, we monitored the SLB-formation process by ellipsometry. As this optical technique senses the dry mass, net desorption of material would be directly detected as an increase in the ellipsometric angle Δ. After interrupting the SLB-formation process at a lipid coverage corresponding to ~30% of a complete SLB (Fig. 2 *D*), Δ remained stable, confirming that lipid material did not desorb. Therefore, we interpret the QCM-D response after the rinsing step as shown in Fig. 2 *A* as due to the decomposition of surface-bound vesicles into bilayer patches, the increase in frequency, and the decrease in dissipation being caused by the loss of water associated with and the changes in the rigidity of the lipid structures. Consequently, the QCM-D data indicate that the typical time for the spontaneous transition of isolated mica-bound vesicles into bilayer patches is in the range of minutes to hours. This is a remarkable difference compared to isolated vesicles on silica that remained stable over days under identical conditions (Richter et al., 2003).

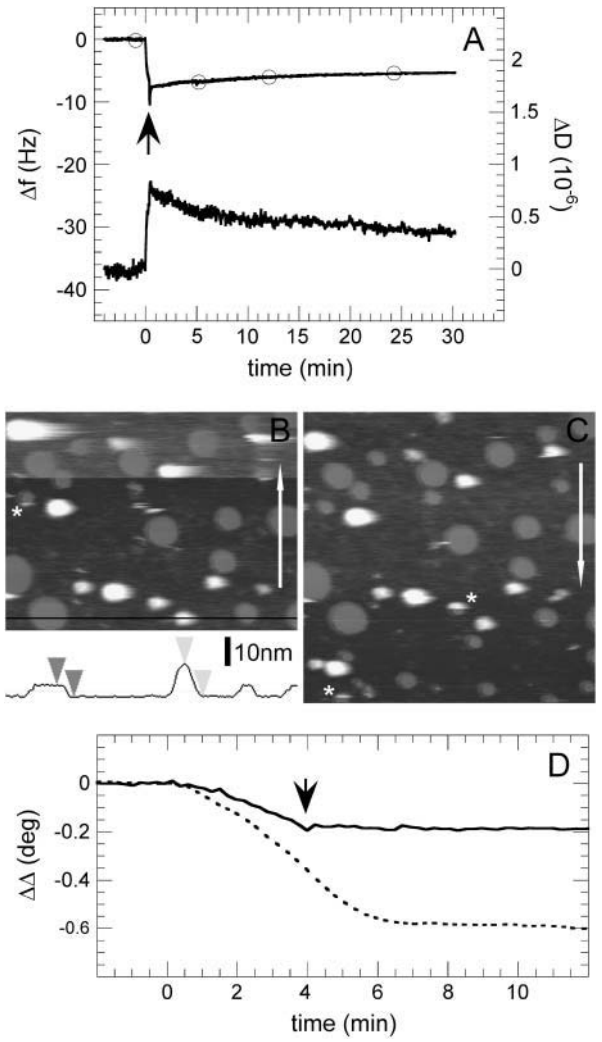

FIGURE 2 SLB formation from ~10 μg/mL SUVs made of DOPC/DOPS (4:1) interrupted at an early stage. (*A*) QCM-D response (frequency, Δf (–○–), and dissipation, ΔD (*solid line*), at 25 MHz); after the rinse (*arrow*), the adsorbed vesicles are not stable. (*B* and *C*) Two sequential images recorded after transfer of the mica-coated QCM-D sensor to the AFM; vesicles and bilayer patches, identified by their height and shape (cross section in *inset*, *gray* and *black arrowheads*, respectively) coexist. A few vesicles (*asterisks*) become ruptured by the influence of the AFM tip. Image size (*z*-scale), 1 mm (20 nm); the slow scan direction (contact mode) is indicated (*arrows*). The asymmetric and varying shape of individual vesicles is due to very low and slightly varying scanning forces (see Supplementary Material). (*D*) Changes in the ellipsometric angle, $\Delta\Delta$; after the rinse (*solid line*, *arrow*) at $\Delta\Delta = -0.18°$, corresponding to 30% of a complete SLB, the signal remains stable confirming that lipid material is not desorbing. For comparison, the response for the formation of a complete SLB is shown (*dotted line*), resulting in $\Delta\Delta = -0.6°$. Lipid deposition for the ellipsometry measurements was performed at concentrations of ~5 μg/mL (*solid line*) and ~10 μg/mL (*dotted line*), respectively.

Stability and mobility of small SLB patches

To investigate the stability of bilayer patches, a certain area was imaged repetitively with varying forces (Fig. 3). Although almost all SLB patches remained immobile and kept their initial shape, connections between a few distant patches (*asterisks* in Fig. 3 *B*) were established, likely induced by the AFM tip that was temporarily operated at an elevated force. The resulting patches clearly reshaped into circular objects (Fig. 3 *C*), the area of which corresponded to the sum of the areas of the initial patches, confirming that coalescence events were tracked (for details see the Supplementary Material). The center of mass of the merging patches remained approximately fixed during the merger event (Fig. 3 *B*). Given the image acquisition time of ~2 min and the fact that connections are visible over several scan lines, corresponding to ~0.2 s each, the time needed for coalescence and reshaping can be estimated to be in the range of a few seconds to a few minutes. We note that, in contrast to our observation on mica, small SLB patches of stable noncircular shape were observed on silica (Richter et al., 2003).

The lateral movement of lipid material associated with the coalescence of two patches (Fig. 4 *A*) can trigger a cascade of subsequent events of coalescence with other neighboring patches (Fig. 4, *B–D*), leading to substantial modifications in the organization of the surface-bound lipid material. It is easily conceivable that also intact adsorbed vesicles can be ruptured by contact with the approaching active edge of a neighboring bilayer patch. Shape changes due to coalescence can thus play a significant role in the organization of lipid material during the SLB-formation process.

The late phase of SLB formation

Fig. 5 *A* demonstrates that after rinsing at a later stage, i.e., shortly after the minimum in frequency and the maximum in dissipation are reached, a considerable rearrangement of the surface-bound lipid material takes place within minutes. In the absence of vesicles in solution, Δf increased above -25 Hz (to -16 Hz) and ΔD decreased to 0.4×10^{-6}, indicating that the major part of adsorbed vesicular material was transformed into bilayer patches. Corresponding AFM images showed indeed extended domains of lipid bilayers coexisting with a small number of vesicles (Fig. 5 *B*) and ellipsometry experiments indicated that no significant desorption occurred in similar conditions (Fig. 5 *C*).

Interestingly, noncircularities persisted on large patches, i.e., patches with a radius >200 nm, over times of 1 h and more. Surprisingly, patch boundaries with local radii of curvature <150 nm (*arrowheads* in Fig. 5 *B*) could be found, indicating the presence of forces/obstacles that counteract the shape equilibration that would be expected from minimization of the line tension (Rädler et al., 1995; Muresan and Lee, 2001).

AFM images acquired after interrupting the SLB formation at an even later stage, showed an apparently confluent bilayer in which local defects persisted (Fig. 6 *A*). Elongated defects of several micrometers in length and down to a few nanometers in width could be observed, which were

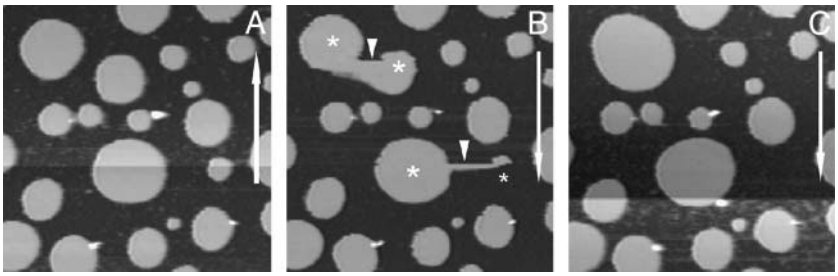

FIGURE 3 Sequential AFM images (contact mode) before (*A*), during (*B*), and after (*C*) the merger of bilayer patches. Images *A* and *C* are scanned at lowest possible forces (~100 pN). In image *B* the force was slightly increased (~300 pN) inducing the merger (*arrowheads*) of several patches (*asterisks*). Before image acquisition, 25 μg/mL SUVs of DOPC/DOPS (4:1) in 2 mM $CaCl_2$ were incubated for ~1 min and rinsed in buffer. Image size (*z*-scale), 1.25 mm (10 nm); the slow scan direction is indicated (*arrows*). Slight changes in the apparent size of individual patches and variations in the overall contrast (*A* and *C*) are due to slight instantaneous changes in the scanning force (see Supplementary Material).

particularly frequent after incubation with SUV solutions at low concentration (10 mg/mL). Notably, the apparent local radius of curvature of the bilayer boundary at the ends of some of these defects (*arrowheads* in Fig. 6 *A*) was in the range of 10 nm. Given our experimental conditions, we estimate that such small radii are at the limit of resolution. It is therefore not clear, whether the apparent topography reflects a truly continuous bilayer boundary or whether, instead, it marks the endpoint of a zone (*dotted line* in Fig. 6 *A*) at which two patch boundaries appose with each other without coalescing, the gap between them being small enough to remain unresolved by AFM. Whatever the true topography, some of these defects remained stable over hours, again indicating the presence of forces that inhibit shape equilibration (Benvegnu and McConnell, 1992).

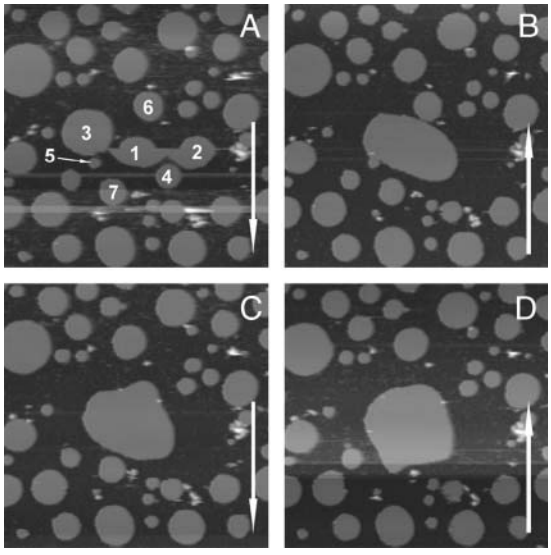

FIGURE 4 Sequential AFM images (contact mode) of coalescence events of bilayer patches. After the tip-induced merger of patches 1–3 (*A*), the coalescence with patches 4 (*B*), 5–6 (*C*), and 7 (*D*) is induced by the movements of the reshaping patch. Before image acquisition, 25 μg/mL SUVs of DOPC/DOPS (4:1) in 2 mM $CaCl_2$ were incubated for ~1 min and rinsed in buffer. Image size (*z*-scale), 1.75 mm (10 nm); the slow scan direction is indicated (*arrows*).

Subsequent reincubation as well as incubation without interruption led to bilayers that were close to defect-free, as seen from the AFM images (Fig. 6 *B*). To verify whether defects persisted that were invisible to AFM, some DOPS-containing bilayers were incubated with the protein annexin A5 and the growth of two-dimensional crystals was followed as described elsewhere (Reviakine et al., 1998). Round-shaped crystals were observed as expected for undisturbed crystal growth (Reviakine et al., 1998) (not shown), whereas elongated discontinuities in the supporting bilayer are expected to locally prevent crystal growth thereby distorting the crystal's shape.

Influence of the vesicle charge and the presence of calcium on the SLB formation on mica

The vesicle charge and the presence of calcium were previously shown to have a pronounced influence on the lipid deposition pathways on silica (Richter et al., 2003). For comparison, we followed the global kinetics of lipid deposition on mica for vesicles of varying charge in the presence of the calcium chelator EDTA and in the presence of 2 mM calcium ions, respectively, by QCM-D. The vesicle charge was varied by mixing appropriate amounts of positively charged (DOTAP), zwitterionic (DOPC), and negatively charged (DOPS) lipids. For a quantitative comparison of the lipid deposition process, the minimum in frequency, Δf_{min}, and the maximum in dissipation, ΔD_{max}, were determined. SLB formation, if occurring, was additionally characterized by the time, t_{SLB}, required to attain stable values in frequency, Δf_{fin}, and dissipation, ΔD_{fin}. Furthermore, the stability of adsorbed isolated vesicles was checked by interrupting the SLB formation at low coverage. Table 1 and Figs. 7 and 8 summarize the obtained results.

In the absence of calcium, SUVs made from DOPC adsorbed to mica (Fig. 7 *B*) but did not rupture at moderate lipid concentrations (100 mg/mL), in agreement with previous studies (Reviakine and Brisson, 2000; Benes et al., 2004). In contrast, SLB formation was observed on silica (Richter et al., 2003). Rather small amounts of negative charges (20% DOPS) were sufficient to completely inhibit

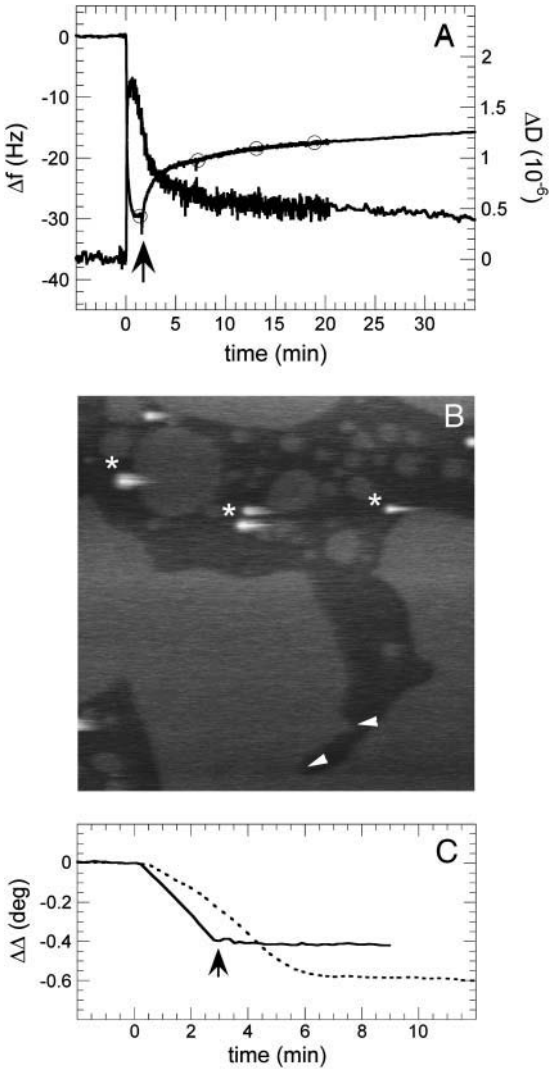

FIGURE 5 SLB formation from ~50 μg/mL SUVs made of DOPC/DOPS (4:1) interrupted at a late stage. (*A*) QCM-D response (frequency, Δf (–○–), and dissipation, ΔD (*solid line*), at 25 MHz); after the rinse (*arrow*) close to the minimum in frequency, surface-bound lipid material undergoes quick structural changes. (*B*) AFM image (tapping mode) taken after the transfer of the sample; extended patches coexist with a few vesicles (*asterisks*). The bilayer patches exhibit edges with small local radius of curvature (<150 nm; *arrowheads*). Image size (*z*-scale), 1.5 mm (20 nm). (*C*) Changes in the ellipsometric angle, $\Delta\Delta$; after rinsing (*solid line, arrow*) at $\Delta\Delta = -0.41°$, corresponding to 68% of a complete SLB, the signal remains stable confirming that lipid material is not desorbing. The response for the formation of a complete SLB is shown for comparison (*dotted line*). Lipid deposition for the ellipsometry measurements was performed at concentrations of ~20 μg/mL (*solid line*) and ~10 μg/mL (*dotted line*), respectively.

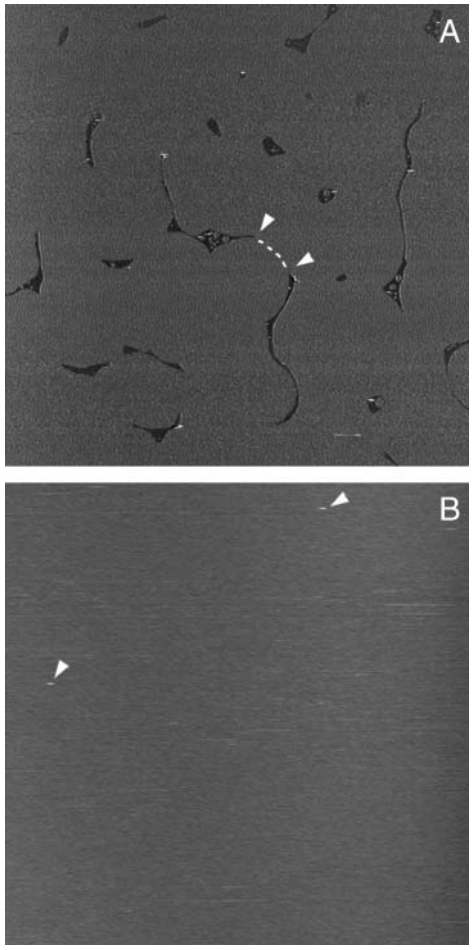

FIGURE 6 (*A*) AFM image of an SLB formed from a solution of 10 mg/mL SUVs made of DOPC/DOPS (4:1) and interrupted at a very late stage (contact mode). Numerous elongated defects persist. The ends of some of these defects (*arrowheads*) appear sharp. It is not clear whether these ends indeed represent a true bilayer boundary with a small but finite radius of curvature (~15 nm). Alternatively, these points may mark the limits of an unresolved gap (*dotted line*) between two bilayer patches. (*B*) AFM image of an SLB formed from a solution of 100 mg/mL SUVs made of DOPC/DOPS (4:1) (tapping mode). The bilayer is ideal without visible defects, except for two protrusions (*arrowheads*), likely to be trapped vesicles. Image size (*z*-scale), 10 mm (10 nm).

lipid adsorption. Similarly, vesicle adsorption was hampered on silica with increasing negative vesicle charge, although inhibition occurred only at considerably higher negative charge (50% DOPS) (Richter et al., 2003). These observations suggest that the electrostatic repulsion between negatively charged vesicles and the support is stronger with mica than with silica. In conjunction, we note that no SLBs could be formed on mica with DOPS-containing SUVs. For comparison, SLB formation was inhibited on silica only at a DOPS content of 33% and more (Richter et al., 2003).

QCM-D responses indicated the formation of SLBs for all types of positively charged SUVs investigated. These observations are qualitatively similar to silica. It is, however, notable that the formation of mica SLBs with pure DOTAP-SUVs (Fig. 7 *C*) exhibited very low dissipation values ($\Delta D_{max} < 0.5 \times 10^{-6}$) throughout the whole SLB-formation process. Corresponding values on silica were slightly higher ($\Delta D_{max} = 0.8 \pm 0.1 \times 10^{-6}$)

TABLE 1 Parameters measured by QCM-D for the deposition of vesicles with varying lipid composition

Lipid ratio										
DOTAP	DOPC	DOPS	[Ca](mM)	Δf_{min}(Hz)	ΔD_{max} (10^{-6})	Δf_{fin}(Hz)	ΔD_{fin}(10^{-6})	t_{SLB}(min)	Vesicle deposition pathway	Stability of vesicles at low coverage
1	–	–	0*	–	0.5	−25	0.2	12	SLB	Fast rupture†
1	4	–	0*	−35	2.7	−27	0.8	3	SLB	No rupture, no desorption
–	1	–	0*	−103	10.0	–	–	–	SVL	No rupture, slow desorption
	9	1	0*	−13	2.0	–	–	–	SVL	–
–	4	1	0*	0	0	–	–	–	No adsorption	–
1	–	–	2	–	0.3	−24	0.2	10	SLB	Fast rupture†
1	4	–	2	−32	1.8	−26.5	0.5	3	SLB	No rupture, no desorption
–	1	–	2	−50	4.0	−25	0	5	SLB	No rupture, no desorption
–	9	1	2	−50	2.6	−25	0	3.3	SLB	–
–	4	1	2	−45	2.5	−26	0.2	3.3	SLB	Slow rupture‡
–	2	1	2	−34	1.7	−25.5	0.2	5	SLB	Slow rupture‡
–	1	1	2	−36	1.5	−25.5	0.2	1.3	SLB	Slow rupture‡
–	1	2	2	−34	1.5	−25.5	0.2	2	SLB	Slow rupture‡
–	1	4	2	−32	1.0	−26	0.2	1.3	SLB	Slow rupture‡

*Measured in the presence of 2 mM EDTA.
†Isolated vesicles rupture within seconds or less after adsorption.
‡Isolated vesicles rupture within minutes or hours after adsorption.

(Richter et al., 2003), indicating that the tendency toward immediate rupture of isolated DOTAP vesicles is even more pronounced on mica.

The formation of a supported vesicular layer (SVL) with DOPC-SUVs (Fig. 7 *B*) deserves some additional attention. The adsorption of these vesicles was partly reversible (Reviakine and Brisson, 2000; Benes et al., 2004), which is exceptional for the vesicle-surface interactions that we have so far investigated on silica and on mica. The frequency shift of $|\Delta f_{min}| = 103$ Hz, indicates a high surface coverage (Keller and Kasemo, 1998). Interestingly, the QCM-D responses after the addition of calcium (Fig. 7 *B*) suggest that the SVL is converted into a complete supported lipid bilayer, even though no vesicles were present in solution. Furthermore, the maximum dissipation shift for the mica-supported vesicular layer, $\Delta D_{max} = 10 \times 10^{-6}$, is remarkably high, resulting in a ratio between dissipation and frequency of $\Delta D_{max}/|\Delta f_{min}| = 0.10 \times 10^{-6} \cdot Hz^{-1}$. This is significantly more than on silica ($0.06 \times 10^{-6} \cdot Hz^{-1}$) (Richter et al., 2003), and indicates that DOPC vesicles become less flattened on mica than on silica (Reimhult et al., 2002b). For simplicity, we have compared the ratio of $\Delta D_{max}/|\Delta f_{min}|$. (Note, however, that in addition to the flattening of the vesicle, the intervesicle interaction at high surface coverage can affect $\Delta D/\Delta f$. This potential artifact can be avoided by comparing the $\Delta D/|\Delta f|$-values at low vesicular coverage (Reimhult et al., 2002b). Corresponding values are $0.14 \times 10^{-6} \cdot Hz^{-1}$ and $0.08 \times 10^{-6} \cdot Hz^{-1}$ (at $n = 7$) on mica and silica, respectively, supporting our conclusions that DOPC vesicles become more flattened on silica.)

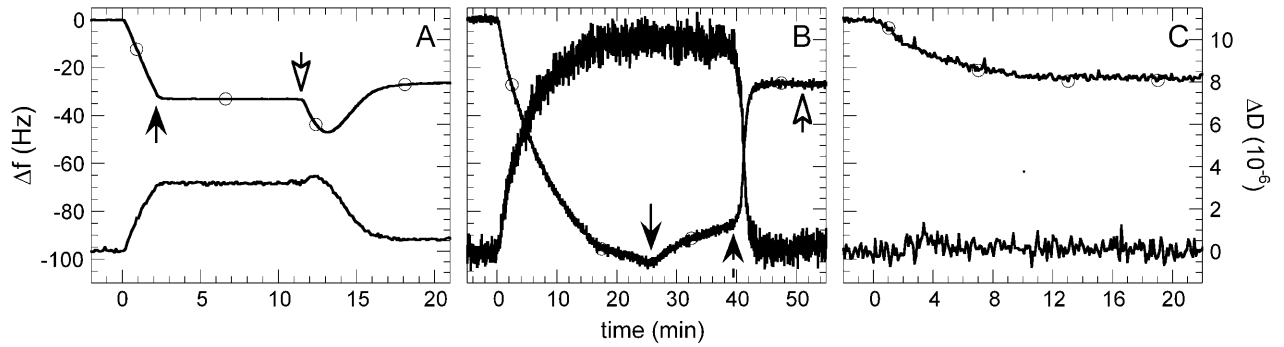

FIGURE 7 QCM-D responses (frequency, Δf (–○–), and dissipation, ΔD (*solid line*)) for the deposition of 0.1 mg/mL SUVs composed of different lipids on mica. Lipid exposure starts at 0 min. (*A*) DOPC in 2 mM $CaCl_2$ (25 MHz, flow mode); after the rinse (*black arrow*) at an early stage of SLB formation, Δf and ΔD remain stable, indicating that adsorbed vesicles are stably bound and neither desorb nor rupture; reincubation with SUVs (*white arrow*) leads to completion of the SLB formation. (*B*) DOPC in 2 mM EDTA (35 MHz, flow mode); formation of an SVL exhibiting high dissipation; a rinse with EDTA-containing buffer (*black arrow*) leads to partial desorption of the vesicles; a rinse with calcium-containing buffer (*black dotted arrow*) leads to the formation of an SLB, as characterized by a frequency shift of −26 Hz and a very low dissipation shift; subsequent addition of SUVs in 2 mM $CaCl_2$ (*white arrow*) does not further affect the SLB. (*C*) DOTAP in 2 mM EDTA (35 MHz, flow mode); formation of an SLB; vesicles rupture instantaneously upon adsorption.

In the presence of calcium, SLBs were formed over the entire range of lipid mixtures investigated. Notably, SLBs could be formed from vesicles containing as much as 80% DOPS. A detailed examination revealed a tendency of t_{SLB} and $|\Delta f_{min}|$ to decrease toward higher negative charges (Fig. 8). This evidences that increasing DOPS content facilitates SLB formation on mica in the presence of calcium. Notably, the opposite was observed on silica. The influence of calcium on the SLB-formation process for DOTAP-containing vesicles was minor.

Isolated mica-bound vesicles that contained only DOPC or small amounts of DOTAP were found to be stable over minutes and hours (Fig. 7 *A*), similar to the results obtained on pure silica (Keller et al., 2000). Isolated vesicles from all lipid mixtures containing 20% and more DOPS, however, slowly but measurably transformed into SLB patches.

Influence of the AFM tip on the imaging of lipid vesicles and SLB patches

Lipid structures such as surface-bound vesicles or bilayer patches are known to be easily modified by interactions with the AFM tip (Jass et al., 2000; Reviakine and Brisson, 2000; Richter and Brisson, 2003; Liang et al., 2004). During initial investigations with nonmodified tips it became apparent that the lipid material can mediate strong tip-sample interactions (Richter and Brisson, 2003), which renders the imaging of heterogeneous lipid structures such as coexisting bilayer patches and vesicles unstable and prone to artifacts, in particular, for low scan speeds and small image sizes. As demonstrated by the AFM images shown here, the modification of the AFM tip with PLL-*g*-PEG resulted in an improved control in imaging such lipid structures down to image sizes of 1 μm and less. When forces exerted by the AFM tip were adjusted to a minimum, vesicles and bilayer patches could be imaged intact (c.f. Fig. 5 *B*). Alternatively, increased forces could be employed to induce the rupture of vesicles (*arrowheads* in Fig. 2, *B* and *C*), the coalescence of bilayer patches (c.f. Figs. 3 and 4), or the displacement of lipid structures (not shown).

Imaging in tapping mode provided least disturbance of the lipid material, though images in contact mode also could be obtained with only minor artifacts, such as occasional tip-induced vesicle rupture. In particular, small bilayer patches appeared (almost) circular and immobile both in tapping and contact mode, indicating that small lateral forces did not significantly alter the location or overall shape of the patches.

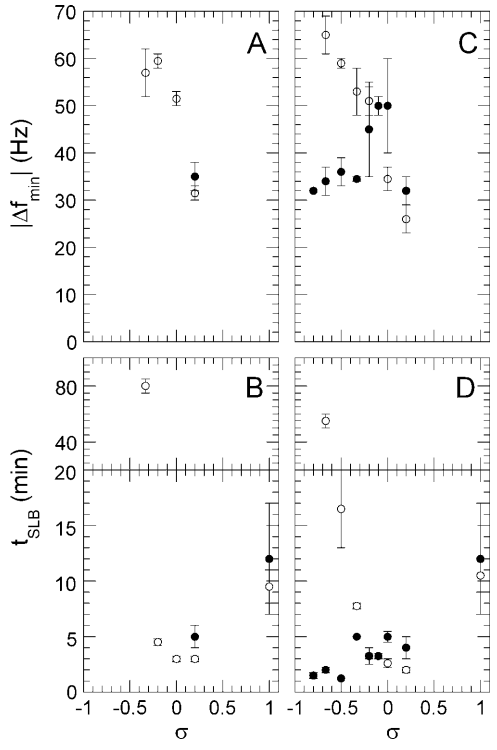

FIGURE 8 The local minimum in frequency, $|\Delta f_{min}|$ (*A* and *C*), and SLB-formation time, t_{SLB} (*B* and *D*), as a function of the fractional lipid charge, σ, ($\equiv$ average number of charges per lipid molecule). Data for mica (●) and silica (○; adapted from Richter et al., 2003) are shown in the presence of 2 mM EDTA (*A* and *B*) and 2 mM calcium (*C* and *D*), respectively. Data are given for lipid mixtures and conditions that lead to SLB formation; $|\Delta f_{min}|$ is indicated only if the SLB formation exhibits a local minimum in frequency.

Effects of the AFM tip on the apparent size of the bilayer patches and vesicles

We observed small but significant variations in the apparent size of the bilayer patches, depending on the applied force (see Supplementary Material). The apparent radius and height of the bilayer patches were observed to decrease by ~5 and 0.2 nm, respectively, when increasing the normal force by ~200 pN from the minimum force required for proper tracking of the surface. Similarly, the height of surface-bound vesicles was observed to vary by a few nanometers. This indicates that the forces exerted by the tip can induce lateral or normal compression of the lipid assemblies (as well as the tip coating). Next to tip-convolution effects, the sample deformation, thus, renders the determination of the correct size of adsorbed vesicles and bilayer patches a complex task, as discussed in the Supplementary Material.

DISCUSSION

In this study, we combine QCM-D, ellipsometry, and AFM to provide a detailed picture of the pathways of deposition of lipid vesicles on mica. Previous experimental (Keller et al., 2000; Reviakine and Brisson, 2000; Johnson et al., 2002; Richter et al., 2003) and theoretical (Seifert and Lipowsky, 1990; Seifert, 1997; Zhdanov et al., 2000) studies have shown that adsorbed lipid vesicles can transform into bilayer patches via at least three different mechanisms: i), spontaneous rupture of isolated vesicles; ii), rupture of

vesicles induced by high vesicle density (critical vesicular coverage); and iii), rupture of vesicles induced by the active edge of a bilayer patch. We show here that, by varying the vesicle composition and the calcium-EDTA balance, all above-described mechanisms can be reproduced on mica, and that significant differences exist between mica and silica.

Rupture of isolated vesicles

The time from adsorption to rupture of isolated vesicles, i.e., surface-bound vesicles at sufficiently low coverage, can vary widely. Whereas we found DOTAP to rupture faster than what can be resolved (~1 s) by the employed techniques, DOPC vesicles were stable (Fig. 7 *A*) in 2 mM $CaCl_2$ over experimental timescales (~1 h). Both extremes can be understood from a thermodynamic perspective of the interaction between vesicle and support and have been described before (Lipowsky and Seifert, 1991; Seifert, 1997; Reviakine and Brisson, 2000).

We report here on an intermediate time range (minutes to hours) that is needed for DOPS-containing vesicles to rupture in the presence of calcium, which highlights the importance of the kinetic perspective (Zhdanov and Kasemo, 2001). The parameters that govern the rupture dynamics remain to be elucidated and will be discussed further below.

Rupture induced by critical vesicular coverage

The pathway of vesicle rupture induced by the cooperative action of neighboring adsorbed vesicles has been described and characterized in detail on silica (Keller et al., 2000; Reimhult et al., 2002a,b; Richter et al., 2003). Similar to silica (Keller et al., 2000), isolated vesicles containing pure DOPC or DOPC/DOTAP (4:1) were observed to be stable when adsorbed on mica in the presence of calcium (c.f. Fig. 7 *A*). The formation of SLBs at higher surface coverage evidences that the influence of neighboring vesicles is necessary to induce the rupture of the first vesicles, indicating that the phenomenon of critical vesicular coverage is also present on mica (Reviakine and Brisson, 2000).

Coexistence of several vesicle rupture mechanisms

Once a few vesicles have ruptured by one of the two above-described mechanisms, further vesicle rupture can also be induced by the active edge of bilayer patches, enhancing the growth of bilayer patches and, eventually, leading to the formation of an SLB.

As mentioned above it takes minutes to hours for isolated DOPS-containing vesicles to rupture (c.f. Fig. 2). On the other hand, the time needed to form an SLB is in the range of a few minutes with the employed lipid concentration (~100 μg/mL). This raises the question whether the combination of rupture of isolated vesicles and edge-induced rupture is sufficient to explain the SLB formation at such short timescales. If vesicle adsorption is much faster than the rupture of isolated vesicles, the surface density of intact vesicles may locally become elevated. This suggests in alternative that rupture induced via the critical vesicular coverage coexists with the rupture of isolated vesicles. Future theoretical treatments, similar to the ones described earlier by Zhdanov et al. (2000) may allow distinguishing between these two scenarios. Also, as the time needed to establish the critical vesicular coverage is dependent on the bulk lipid concentration, this experimental parameter provides the means for controlling the balance between the rupture of isolated vesicles and rupture induced by the critical vesicular coverage.

We note that the presence of a local minimum in frequency and a local maximum in dissipation, as commonly observed by QCM-D, is a necessary but not a sufficient condition to identify the critical vesicular coverage as the unique mechanism for the formation of the first bilayer patches. Additional AFM imaging, allowing for the examinations on the level of a single vesicle, or interrupted QCM-D measurements, allowing for the investigation of the overall stability of the adsorbed lipid material, are required to ascertain that the critical vesicular coverage is the only rupture-initiating mechanism present.

The role of shape changes in bilayer patches

AFM data indicate that the interactions between lipids and the mica support are sufficiently strong in order for SLB patches and bound vesicles to be stably located in the presence of small and transient forces. On the other hand, the interactions are sufficiently weak to allow for movements and/or reshaping in the presence of permanent forces, such as the line tension of small noncircular patches (c.f. Fig. 3) (Muresan and Lee, 2001). This sliding motion has important consequences, as reshaping patches can catalyze mergers with neighboring patches (c.f. Fig. 4) or vesicles and thereby enhance vesicle rupture via active bilayer edges.

It may be tempting to postulate that such an effect can be of considerable value to fill up defects in the bilayer during the final stage of SLB formation. In the light of our observation that the propensity for shape changes is decreased (at least locally) at higher coverage (Fig. 6 *A*) such a conclusion appears premature. However, as demonstrated earlier for silica (Richter et al., 2003), close to defect-free SLBs can be formed without reshaping being present. A potential origin for the decreased speed of shape relaxation may be the presence of contaminations in the bilayer or on the solid support.

Taken together, our results demonstrate that the timescales associated with the different mechanisms of vesicle rupture can vary. As the mechanisms of vesicle rupture can coexist and exhibit some degree of interdependence, a multitude of SLB-formation pathways can occur.

Comparing silica and mica: the role of calcium

We observed several pronounced differences in the deposition of lipid vesicles and in the SLB formation on mica and silica supports, despite the fact that both supports are highly hydrophilic and usually possess an overall negative charge. (Surface charges ~0.1 electron per nm^2 have been reported for both mica (Pashley, 1981a,b) and silica (Bolt, 1957; Considine and Drummond, 2001), with significant variations as a function of electrolyte concentration, pH, and surface preparation (Toikka and Hayes, 1997; Morigaki et al., 2002; Penfold et al., 2002).) For simplicity, we distinguish two situations, namely the absence and the presence of calcium.

In the absence of calcium, repulsive interactions between the negatively charged support and the negatively charged vesicles as well as attractive interactions between the support and positively charged vesicles are stronger on mica than on silica. This underlines the important role of electrostatic interactions and suggests that mica may be more strongly negatively charged than silica.

We found that vesicles made of DOPC become less flattened on mica than on silica. In opposition, the attractive van der Waals forces are expected to be higher on mica than on silica. (Nonretarded Hamaker constants of $A = 2 \times 10^{-20}$ J and 0.8×10^{-20} J have been reported for two surfaces of mica and silica, respectively, interacting in water (Israelachvili, 1992).) This may indicate that electrostatic double layer forces are sufficiently strong to outweigh the van der Waals forces, despite the small surface potential of DOPC under the employed conditions (Egawa and Furusawa, 1999). Alternatively, additional short-ranged forces may substantially influence the vesicle-support interaction. (Silica and mica are known to exhibit remarkable differences in their short-range interactions (Chapel, 1994; Israelachvili and Wennerström, 1996) the molecular origin of which is still under debate.) Although it remains difficult to identify the exact nature of the interaction forces, this example is illustrative for the complexity of the vesicle-support interactions.

The presence of calcium has a remarkable effect on the lipid deposition on mica as evidenced by the fact that SLBs can be formed at a DOPS content of 80% and more (Reviakine et al., 2001; Richter and Brisson, 2004). Recent results (Richter et al., 2005) indicate that, during SLB formation, DOPS molecules become distributed asymmetrically between the two SLB leaflets. Calcium's exceptional capacity to promote SLB formation correlates, thus, with our finding that DOPS molecules become enriched in the SLB's mica-facing side, suggesting the presence of a particular calcium-mediated interaction between mica and DOPS. It is tempting to identify the (re)distribution of DOPS within and in between (flip-flop) the leaflets of adsorbed vesicles as the determining parameter for the slow rupture kinetics that we observed for isolated DOPS-containing vesicles. Interestingly, Yaroslavov et al. (1994, 1998) have reported that a membrane-binding polycationic polymer can induce the redistribution of negatively charged lipids toward the outer leaflet of SUVs, although the mechanism of this polycation-induced flip-flop remains little understood. It appears conceivable that the calcium-mediated interaction between mica and DOPS, in conjunction with the stress that other vesicle-support interactions exert on the vesicle, may enhance lipid flip-flop in mica-bound vesicles, thereby promoting their rupture.

We note that the SLB-promoting effect of calcium is not restricted to DOPS but extends also to DOPC. Although calcium was observed to facilitate adsorption and SLB formation on silica, too, the effect was considerably less pronounced.

Mica-bound lipid material retained some degree of mobility, whereas bilayer patches were found to be immobile on silica. Could a difference in the roughness of the two supports explain this effect (Rädler et al., 1995)? The roughness of silica wafers employed in the reference study (Richter et al., 2003), was in the range of 0.1 nm (Richter and Brisson, 2003), i.e., well below what is generally considered the thickness of the water layer between the lipids and the solid support (Bayerl and Bloom, 1990; Johnson et al., 1991). We therefore refrain from attributing the observed differences entirely to roughness. Other effects may be induced by the nature of the interactions between the solid support and bilayer patches and/or their boundary.

This study, thus, underlines the important role of the solid support in determining the lipid deposition pathway. Whereas the investigations undertaken in this work identified important parameters that determine the lipid deposition pathway, the results also indicate that the interaction between lipids or lipid assemblies and the solid support can be rather complex. It is hoped that further detailed comparative studies on mica, silica, and other surfaces (such as titanium oxide) at varying ionic strength and calcium content will provide access to information on the quantitative as well as molecular level. In particular, such investigations may help to separate the contribution of vesicle-support, intervesicle and intrabilayer interactions, respectively, in the lipid deposition process and, in particular, to elucidate the molecular nature of the calcium-mediated interaction between DOPS and the support.

Combining QCM-D, AFM, and ellipsometry

We emphasize the importance of combining QCM-D, ellipsometry, and AFM to obtain the results reported in this study. The application of all techniques on an identical support allowed obtaining kinetic information about the adsorption, desorption, and rupture of vesicles with high time resolution as well as detailed information about local structural changes of the lipid assemblies. While the multi-technique approach gives an improved control over possible experimental artifacts, the combination on an identical

support opens up for a detailed quantitative investigation of SLB formation or other self-assembly processes.

Influences of the AFM tip on the appearance of immobilized vesicles and SLB patches

The modification of the AFM tip with a lipid-repelling polymer proved essential to reproducibly obtain images of different coexisting lipid structures. Both SLB patches and vesicles could be imaged stably and without lateral displacement. Furthermore, controlled tip forces allowed investigating shape transitions such as patch movement, coalescence or vesicle rupture. Such events can potentially be exploited to quantify the influence of the tip on the apparent size of surface-bound vesicles and bilayer patches. In particular, the coalescence of patches can be exploited to determine the correct size of bilayer patches, and the rupture of adsorbed, flattened vesicles can be used to estimate the diameter of the corresponding nonflattened vesicle as well as to evaluate the influence of the tip on the apparent width of a vesicle (see Supplementary Material).

CONCLUSION AND PERSPECTIVES

The combination of QCM-D, AFM, and ellipsometry has allowed identifying and characterizing a multitude of processes that take place from the adsorption of vesicles to the formation of a complete SLB on mica. Although most of these processes act locally, their interdependence and kinetics determine together the overall dynamics of the SLB-formation process.

Our study provides evidence for important differences in the interaction of lipids with silica and mica, stressing the importance of the solid support, the calcium-EDTA balance, and electrostatic interactions in the SLB-formation process.

The improved imaging of surface-confined lipid structures demonstrated in this study together with the exploitation of the shape transitions (Supplementary Material) for size determinations open up for the reliable quantification of adsorbed lipid material and for the investigation, in detail, of the shape of surface-bound vesicles.

SUPPLEMENTARY MATERIAL

An online supplement to this article can be found by visiting BJ Online at http://www.biophysj.org.

We acknowledge the group of Markus Textor (ETH, Zurich, Switzerland) for providing the PLL-*g*-PEG. We thank Wim Hermens (University of Maastricht, The Netherlands) for providing access to the ellipsometer as well as Aleš Benda and Martin Beneš (Heyrovský Institute, Prague, Czech Republic) for help with its setup. We acknowledge Sylvie Bordère (ICMCB, Bordeaux, France) and Ilya Reviakine (Technical University Clausthal, Clausthal-Zellerfeld, Germany) for discussions around the shape of confined bilayer patches and the SLB-formation process, respectively.

Ralf Richter was partly supported by the CNRS, the Ministère délégué à la Recherche (France), the Conseil Régional d'Aquitaine (France), and by European Community grant FP6-NMP4-CT2003-505868 ''Nanocues''. This research was supported by the Conseil Régional d'Aquitaine, the Fonds Européen de Développement Régional, and European Community grant FP6-NMP4-CT2003-505868 ''Nanocues''.

REFERENCES

Bayerl, T. M., and M. Bloom. 1990. Physical properties of single phospholipid bilayers adsorbed to micro glass beads. A new vesicular model system studied by ^{2}H-nuclear magnetic resonance. *Biophys. J.* 58:357–362.

Benes, M., D. Billy, A. Benda, H. Speijer, M. Hof, and W. T. Hermens. 2004. Surface-dependent transitions during self-assembly of phospholipid membranes on mica, silica, and glass. *Langmuir.* 20:10129–10137.

Benes, M., D. Billy, W. T. Hermens, and M. Hof. 2002. Muscovite (mica) allows the characterization of supported bilayers by ellipsometry and confocal fluorescence correlation spectroscopy. *Biol. Chem.* 383:337–341.

Benvegnu, D. J., and H. M. McConnell. 1992. Line tension between liquid domains in lipid monolayers. *J. Phys. Chem.* 96:6820–6824.

Bolt, G. H. 1957. Determination of the charge density of silica sols. *J. Phys. Chem.* 61:1166–1169.

Boxer, S. G. 2000. Molecular transport and organization in supported lipid membranes. *Curr. Opin. Chem. Biol.* 4:704–709.

Chapel, J.-P. 1994. Electrolyte species dependent hydration forces between silica surfaces. *Langmuir.* 10:4237–4243.

Considine, R. F., and C. J. Drummond. 2001. Surface roughness and surface force measurement: a comparison of electrostatic potentials derived from atomic force microscopy and electrophoretic mobility measurements. *Langmuir.* 17:7777–7783.

Corsel, J. W., G. M. Willems, J. M. M. Kop, P. A. Cuypers, and W. T. Hermens. 1986. The role of intrinsic binding rate and transport rate in the adsorption of prothrombin, albumin and fibrinogen to phospholipid bilayers. *J. Colloid Interface Sci.* 111:544–554.

Cuypers, P. A., J. W. Corsel, M. P. Janssen, J. M. M. Kop, W. T. Hermens, and H. C. Hemker. 1983. The adsorption of prothrombin to phosphatidylserine multilayers quantitated by ellipsometry. *J. Biol. Chem.* 258:2426–2430.

Egawa, H., and K. Furusawa. 1999. Liposome adhesion on mica surface studied by atomic force microscopy. *Langmuir.* 15:1660–1666.

Huang, N.-P., J. Vörös, S. M. De Paul, M. Textor, and N. D. Spencer. 2002. Biotin-derivatized poly (L-lysine)-*g*-poly (ethylene glycol): a novel polymeric interface for bioaffinity sensing. *Langmuir.* 18:220–230.

Israelachvili, J. N. 1992. Intermolecular and Surface Forces. Academic Press, London, UK.

Israelachvili, J., and H. Wennerström. 1996. Role of hydration and water structures in biological and colloidal interactions. *Nature.* 379:219–225.

Jass, J., T. Tjärnhage, and G. Puu. 2000. From liposomes to supported, planar bilayer structures on hydrophilic and hydrophobic surfaces: an atomic force microscopy study. *Biophys. J.* 79:3153–3163.

Johnson, J. M., H. Taekijp, S. Chu, and S. G. Boxer. 2002. Early steps of supported bilayer formation probed by single vesicle fluorescence assays. *Biophys. J.* 83:3371–3379.

Johnson, S. J., T. M. Bayerl, D. C. McDermott, W. A. Adam, A. R. Rennie, R. K. Thomas, and E. Sackmann. 1991. Structure of an adsorbed dimyristoylphosphatidylcholine bilayer measured with specular reflection of neutrons. *Biophys. J.* 59:289–294.

Kam, L., and S. G. Boxer. 2003. Spatially selective manipulation of supported lipid bilayers by laminar flow: steps toward biomembrane microfluidics. *Langmuir.* 19:1624–1631.

Keller, C. A., K. Glasmästar, V. P. Zhdanov, and B. Kasemo. 2000. Formation of supported membranes from vesicles. *Phys. Rev. Lett.* 84:5443–5446.

Keller, C. A., and B. Kasemo. 1998. Surface specific kinetics of lipid vesicle adsorption measured with a quartz crystal microbalance. *Biophys. J.* 75:1397–1402.

Larsson, C., M. Rodahl, and F. Höök. 2003. Characterization of DNA immobilization and subsequent hybridization on a 2D arrangement of streptavidin on a biotin-modified lipid bilayer supported on SiO_2. *Anal. Chem.* 75:5080–5087.

Liang, X., G. Mao, and K. Y. S. Ng. 2004. Probing small unilamellar EggPC vesicles on mica surface by atomic force microscopy. *Colloids Surf. B. Biointerfaces.* 34:41–51.

Lipowsky, R., and U. Seifert. 1991. Adhesion of vesicles and membranes. *Mol. Crys. Liq. Cryst. Sci. Technol.*202:17–25.

McConnell, H. M., T. H. Watts, R. M. Weis, and A. A. Brian. 1986. Supported planar membranes in studies of cell-cell recognition in the immune system. *Biochim. Biophys. Acta.* 864:95–106.

Milhiet, P. E., M.-C. Giocondi, O. Baghdadi, F. Ronzon, B. Roux, and C. le Grimellec. 2002. Spontaneous insertion and partitioning of alkaline phosphatase into model lipid rafts. *EMBO Rep.* 3:485–490.

Morigaki, K., T. Baumgart, U. Jonas, A. Offenhäuser, and W. Knoll. 2002. Photopolymerization of diacetylene lipid bilayers and its application to the construction of micropatterned biomimetic membranes. *Langmuir.* 18:4082–4089.

Muresan, A. S., and K. Y. C. Lee. 2001. Shape evolution of lipid bilayer patches adsorbed on mica: an atomic force microscopy study. *J. Phys. Chem. B.* 105:852–855.

Nollert, P., H. Kiefer, and F. Jähnig. 1995. Lipid vesicle adsorption versus formation of planar bilayers on solid surfaces. *Biophys. J.* 69:1447–1455.

Pashley, R. M. 1981a. DLVO and hydration forces between mica surfaces in Li^+, Na^+, K^+ and Cs^+ electrolyte solutions: a correlation of double-layer and hydration forces with surface cation exchange properties. *J. Colloid Interface Sci.* 83:531–546.

Pashley, R. M. 1981b. Hydration forces between mica surfaces in aqueous electrolyte solutions. *J. Colloid Interface Sci.* 80:153–162.

Penfold, J., E. Staples, and I. Tucker. 2002. On the consequences of surface treatment on the adsorption of nonionic surfactants at the hydrophilic silica-solution interface. *Langmuir.* 18:2967–2970.

Rädler, J., H. Strey, and E. Sackmann. 1995. Phenomenology and kinetics of lipid bilayer spreading on hydrophilic surfaces. *Langmuir.* 11:4539–4548.

Reimhult, E., F. Höök, and B. Kasemo. 2002a. Temperature dependence of formation of a supported phospholipid bilayer from vesicles on SiO_2. *Phys. Rev. E* 66:051905–051901–051904.

Reimhult, E., F. Höök, and B. Kasemo. 2002b. Vesicle adsorption on SiO_2 and TiO_2: dependence on vesicle size. *J. Chem. Phys.* 117:7401–7404.

Reimhult, E., F. Höök, and B. Kasemo. 2003. Intact vesicle adsorption and supported biomembrane formation from vesicles in solution: influence of surface chemistry, vesicle size, temperature and osmotic pressure. *Langmuir.* 19:1681–1691.

Reviakine, I., W. Bergsma-Schutter, and A. Brisson. 1998. Growth of protein 2-D crystals on supported planar lipid bilayers imaged in situ by AFM. *J. Struct. Biol.* 121:356–361.

Reviakine, I., A. Bergsma-Schutter, A. N. Morozov, and A. Brisson. 2001. Two-dimensional crystallization of annexin A5 on phospholipid bilayers and monolayers: a solid-solid phase transition between crystal forms. *Langmuir.* 17:1680–1686.

Reviakine, I., and A. Brisson. 2000. Formation of supported phospholipid bilayers from unilamellar vesicles investigated by atomic force microscopy. *Langmuir.* 16:1806–1815.

Reviakine, I., and A. Brisson. 2001. Streptavidin 2D crystals on supported phospholipid bilayers: towards constructing anchored phospholipid bilayers. *Langmuir.* 17:8293–8299.

Richter, R. P., and A. Brisson. 2003. Characterization of lipid bilayers and protein assemblies supported on rough surfaces by atomic force microscopy. *Langmuir.* 19:1632–1640.

Richter, R. P., and A. Brisson. 2004. QCM-D on mica for parallel QCM-D–AFM studies. *Langmuir.* 20:4609–4613.

Richter, R. P., N. Maury, and A. Brisson. 2005. On the effect of the solid support on the inter-leaflet distribution of lipids in supported lipid bilayers. *Langmuir.* 21:299–304.

Richter, R. P., A. Mukhopadhay, and A. Brisson. 2003. Pathways of lipid vesicle deposition on solid surfaces: a combined QCM-D and AFM study. *Biophys. J.* 85:3035–3047.

Rodahl, M., F. Höök, A. Krozer, P. Brzezinski, and B. Kasemo. 1995. Quartz crystal microbalance setup for frequency and Q-factor measurements in gaseous and liquid environments. *Rev. Sci. Instrum.* 66:3924–3930.

Sackmann, E. 1996. Supported membranes: scientific and practical applications. *Science.* 271:43–48.

Salafsky, J., J. T. Groves, and S. G. Boxer. 1996. Architecture and function of membrane proteins in planar supported bilayers: a study with photosynthetic reaction centers. *Biochemistry.* 35:14773–14781.

Sauerbrey, G. 1959. Verwendung von Schwingquartzen zur Wägung dünner Schichten und zur Mikrowägung. [in German]. *Z. Phys.* 155:206–222.

Seantier, B., C. Breffa, O. Félix, and G. Decher. 2004. In situ investigations of the formation of mixed supported lipid bilayers close to the phase transition temperature. *Nano Lett.* 4:5–10.

Seifert, U. 1997. Configuration of fluid membranes and vesicles. *Adv. Phys.* 46:13–137.

Seifert, U., and R. Lipowsky. 1990. Adhesion of vesicles. *Phys. Rev. A.* 42:4768–4771.

Starr, T. E., and N. L. Thompson. 2000. Formation and characterization of planar phospholipid bilayers supported on TiO2 and SrTiO3 single crystals. *Langmuir.* 16:10301–10308.

Toikka, G., and R. A. Hayes. 1997. Direct measurement of colloidal forces between mica and silica in aqueous electrolyte. *J. Colloid Interface Sci.* 191:102–109.

Tokumasu, F., A. J. Jin, G. W. Feigenson, and J. A. Dvorak. 2003. Atomic force microscopy of nanometric liposome adsorption and nanoscopic membrane domain formation. *Ultramicroscopy.* 97:217–227.

Tompkins, H. G. 1993. A User's Guide to Ellipsometry. Academic Press, London, UK.

Watts, T. H., A. A. Brian, J. W. Kappler, P. Marrack, and H. M. McConnell. 1984. Antigen presentation by supported planar membranes containing affinity-purified I-Ad. *Proc. Natl. Acad. Sci. USA.* 81:7564–7568.

Yaroslavov, A. A., E. A. Kiseliova, O. Y. Udalykh, and V. A. Kabanov. 1998. Integrity of mixed liposomes contacting a polycation depends on the negatively charged lipid content. *Langmuir.* 14:5160–5163.

Yaroslavov, A. A., V. E. Kul'kov, A. S. Polinsky, B. A. Baibakov, and V. A. Kabanov. 1994. A polycation causes migration of negatively charged phopholipids from the inner to outer leaflet of the liposomal membrane. *FEBS Lett.* 340:121–123.

Yip, C. M., A. A. Darabie, and J. McLaurin. 2002. Ab42-peptide assembly on lipid bilayers. *J. Mol. Biol.* 318:97–107.

Zhdanov, V. P., and B. Kasemo. 2001. Comments on rupture of adsorbed vesicles. *Langmuir.* 17:3518–3521.

Zhdanov, V. P., C. A. Keller, K. Glasmästar, and B. Kasemo. 2000. Simulation of adsorption kinetics of lipid vesicles. *J. Chem. Phys.* 112: 900–909.